Including magnetism in an equatorial model for asteroseismology

M. Bentegeat[1,2]
S.N. Breton[1], D. Meduri[1], S. Mathis[3], C. Pezzotti[4]

1 INAF – Osservatorio Astrofisico di Catania, Italy
2 Ecole Polytechnique, Institut Polytechnique de Paris, 91128 Palaiseau, France
3 Université Paris-Saclay, Université Paris Cité, CEA, CNRS, AIM, 91191 Gif-sur-Yvette, France
4 INAF-IAPS, Via del Fosso del Cavaliere 100, 00133 Rome, Italy

1. Magnetism in solar-type stars

Internal magnetism may be responsible for the transport of **angular momentum** from the core of solar-type stars to their outer layers [1,2,3,4] .

Asteroseismology, the study of stellar oscillations, allows us to directly **probe** the dynamics of stellar interiors. In this context, magnetic fields have been characterised in red giants thanks to **perturbative** methods [11,5].

We now need **non-perturbative** approaches to evaluate the impact of **strong fields** [14]. We therefore develop an **equatorial formalism** including the complete **Lorentz force**.

2. Toroidal magnetic field in an equatorial model

$$\partial_r W' = \left(\frac{N^2}{g} + \frac{m\mathcal{B}}{r\mathcal{A}}\right) W' + \left(\mathcal{A} - \frac{\mathcal{B}^2}{\mathcal{A}} - N^2\right) \xi_r$$

$$\partial_r \xi_r = \left(\frac{\tilde{l}(\tilde{l}+1)}{r^2\mathcal{A}} - \frac{1}{c_s^2}\right) W' - \left(\frac{2}{r} + \frac{d\ln\bar{\rho}}{dr} + \frac{N^2}{g} + \frac{m\mathcal{B}}{r\mathcal{A}}\right) \xi_r$$

- Magnetism constants[6], with **Alfvén frequency** and ***m***

$$\mathcal{A} = \sigma_s^2 - m^2\omega_A^2$$
$$\mathcal{B} = 2(\Omega_s\sigma_s + m\omega_A^2)$$

- Restriction of the problem to the **equatorial plane** and to a **toroidal axisymmetric field**
- Cutoff frequency when $\mathcal{A}$=0 (Alfvén wall) [7]

3. Magneto-gravito-inertial waves in PMS stars

- **Scaling the equation** using the constants y_1 and y_2 [8]:

$$y_1 = \frac{\xi_r}{r}x^{2-\tilde{l}} \quad y_2 = \frac{W'}{gr}x^{2-\tilde{l}}$$

$$x\frac{dy_1}{dx} = \left[V_g - \tilde{l} - 1 - m\frac{\bar{\mathcal{B}}}{\bar{\mathcal{A}}}\right] y_1 + \left[\frac{\tilde{l}(\tilde{l}+1)}{C\bar{\mathcal{A}}} - V_g\right] y_2$$

$$x\frac{dy_2}{dx} = \left[C\left(\bar{\mathcal{A}} - \frac{\bar{\mathcal{B}}^2}{\bar{\mathcal{A}}}\right) - A^*\right] y_1 + \left[A^* + m\frac{\bar{\mathcal{B}}}{\bar{\mathcal{A}}} - \tilde{l} + 3 - U\right] y_2$$

- Implementation of the **new formalism** in the **mascaret** code [9]

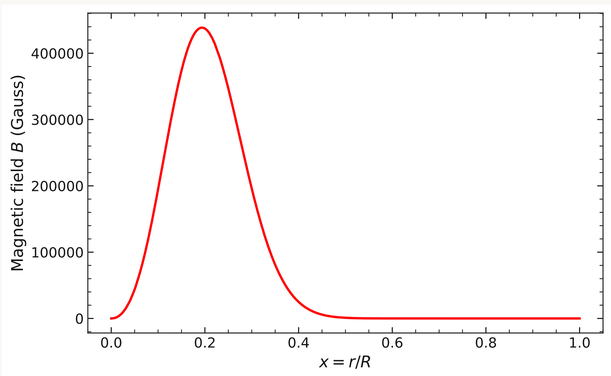

Figure 1 : Radial profile of the field intensity considered in the mascaret computations.

- Effect of a strong toroidal magnetic field with a **Gaussian** radial profile and maximum intensity of 0.45M Gauss.

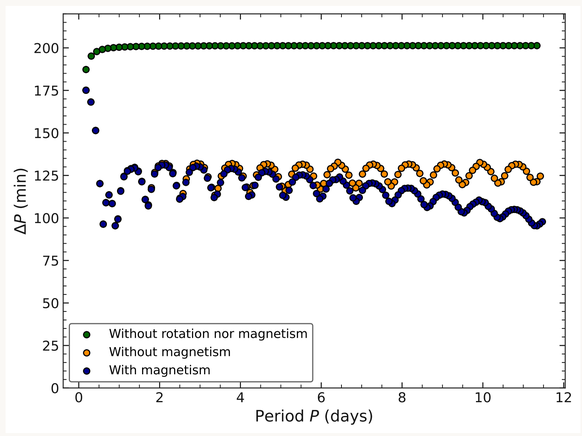

Figure 2 : ΔP vs P diagram for the l = m = 1 modes in the 0.5 Msun PMS model in the co-rotating frame. The dots correspond to the modes computed, with the case without magnetism nor rotation in green, with rotation and without magnetism in orange, and with rotation and magnetism in blue.

- Modes are shifted towards smaller periods: the period spacing **ΔP decreases**
- Greater impact on **lower frequencies**
- In the equations and **JWKB approximation**, ΔP decreases as P, m or B increases, reaching the Alfvén wall and suppressing the waves

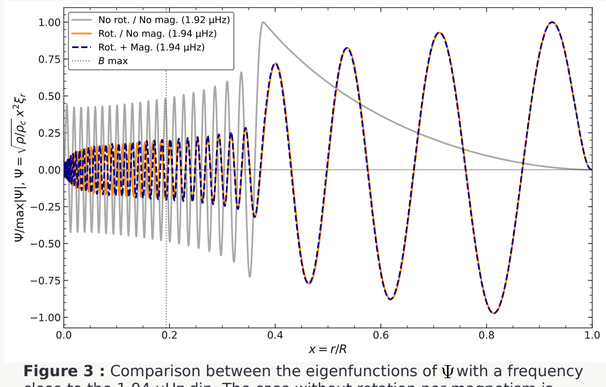

Figure 3 : Comparison between the eigenfunctions of Ψ with a frequency close to the 1.94 μHz dip. The case without rotation nor magnetism is represented in orange, with rotation and without magnetism in orange and with rotation and magnetism in blue. The maximum of the magnetic field is shown with the dashed grey line.

- **Magnetic perturbations** are localized around the maximum of the **Alfvén frequency**

4. Mixed modes with magnetism in red giants

- Magnetic effects in red giants mixed mode spectrum : **depressed dipole modes** [10] and **asymmetry** in the **splitting** of red giant multiplets [5,11]
- **1 solar-mass** model on the RGB [12]
  $\nu_{max} = 100\mu Hz$
- **MAGIC stellar-core simulations** [13] for realistic magnetic field generated by **Tayler instability**
- The star evolves in a **non-linear** regime and **relaxes** slowly

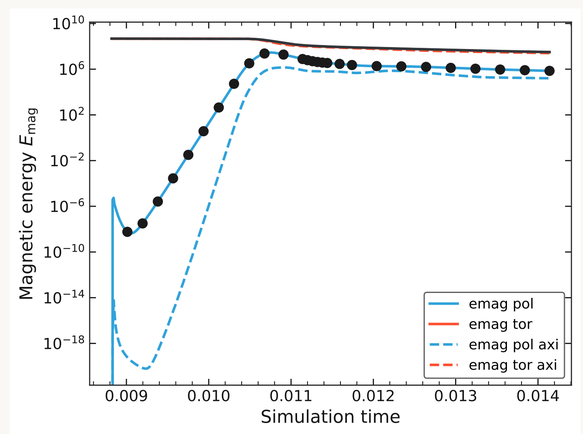

Figure 4 : Evolution of the toroidal, axisymmetric (dotted red) and total (red), and poloidal, axisymmetric (dotted blue) and total (blue), magnetic energy through the simulation. An instability is triggered in a purely toroidal field and the system evolves until a stable state which relaxes slowly. The snapshots from the simulations for which the field is accessible are represented with the black dots.

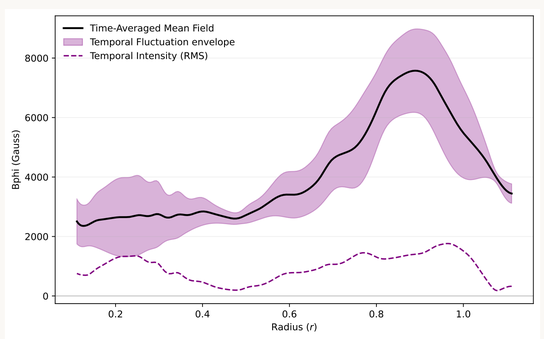

Figure 5 : Average axisymmetric toroidal magnetic field (black) extracted from the simulations in the core of a red giant. The standard deviation is shown with the dotted purple line and represented around the mean field with the purple envelope.

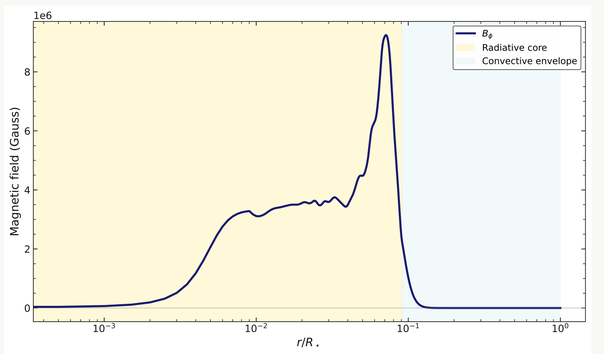

Figure 6 : Magnetic field (blue line) used in the mascaret simulations. It has been chosen to smoothly decrease towards zero magnetic field in the envelope. In yellow is the radiative core of the star, and in blue is the convective envelope.

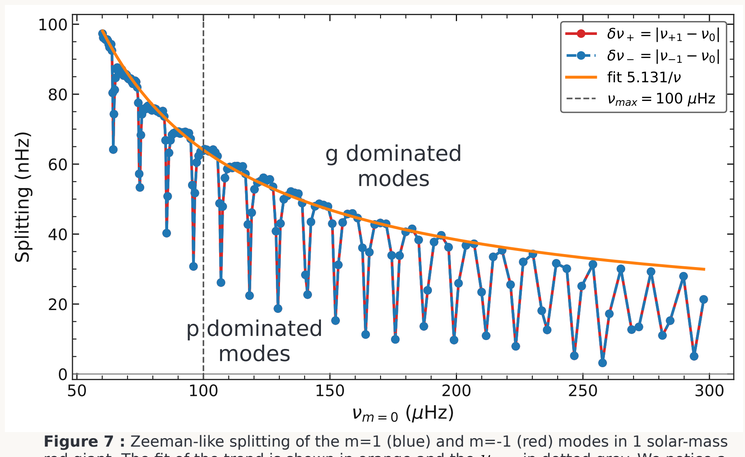

Figure 7 : Zeeman-like splitting of the m=1 (blue) and m=-1 (red) modes in 1 solar-mass red giant. The fit of the trend is shown in orange and the ν_{max} in dotted grey. We notice a dip every 11.2 μHz which coincides exactly with the mixed modes of the star.

- Both *m*=1 and *m*=-1 are **shifted to higher frequencies** in the same way (similarly to Bugnet et al. 2021[11])
- With 4 years of observation, a frequency difference of up to **8 nHz** can be detected
- Toroidal magnetic field detectable from **3M Gauss**
- **Trend** in $1/\nu$ for toroidal field

- MAGIC : **B_{tor}>100 B_r**
  B_r > 30 kG [5] → B_{tor}>3M G, so it could be detected
- The strongest shift in the eigenfunctions is located at the maximum of the magnetic field
- We verify that **g-dominated** modes are more shifted and thus more impacted by magnetism

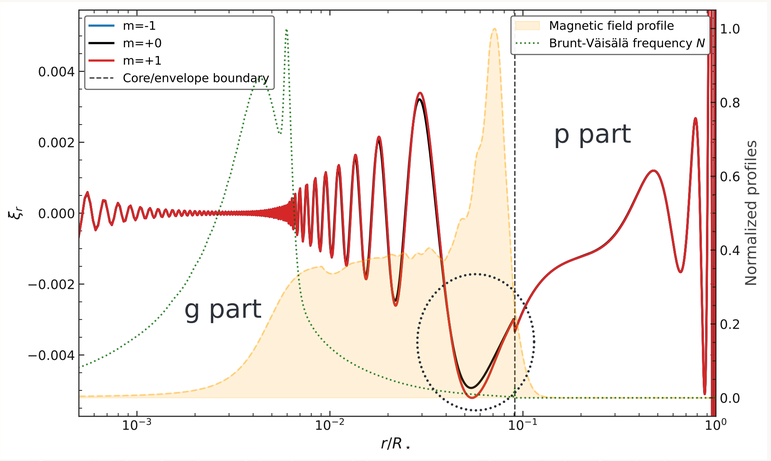

Figure 8 : Eigenfunctions of the closest triplet to nu_max. The m=1 eigenfunction is represented in blue, the m=0 one in black and the m=-1 one in red. The border between the core and the enveloppe is represented with the dotted lines. The magnetic field is shown in yellow and the Brunt-Vaïsälä in dotted green.

Perspectives

- Extending the formalism to a mixed toroidal-poloidal magnetic field
- Comparison between radial and toroidal field effects on observed splittings
- Studying the **interaction between magnetism and rotation** and applying it to other types of stars, e.g. γ-Dor [14,15]
- Investigating the **suppression of modes at lowest frequencies** due to the **Alfvén wall** in the case of an extremely strong field.
- Possible applications to the data collected by ***Kepler***, **TESS** and **PLATO** missions

References

[1] Spruit, H. C. 1999, A&A, 349, 189
[2] Spruit, H. C. 2002, A&A, 381, 923
[3] Eggenberger P., Montalbán J., Miglio A., 2012, A&A, 544, L4
[4] Belkacem K. et al., 2015, A&A, 579, A31
[5] Li, G., Deheuvels, S., Ballot, J., & Lignières, F. 2022, Nature, 610, 43
[6] Mathis, S., & de Brye, N. 2012, A&A, 540, A37
[7] Fuller, J., Piro, A. L., & Jermyn, A. S. 2019, MNRAS, 485, 3661
[8] Townsend, R. H. D., & Teitler, S. A. 2013, MNRAS, 435, 3406
[9] Breton, S. N., Pezzotti, C., Mathis, S., et al. 2026, A&A, 707, L16
[10] Fuller J., Cantiello M., Stello D., Garcia R. A., Bildsten L., 2015, Science, 350, 423
[11] Bugnet, L., Prat, V., Mathis, S., et al. 2021, A&A, 650, A53
[12] Scuflaire, R., Théado, S., Montalbán, J., et al. 2008, Ap&SS, 316, 83
[13] Meduri, D. G., Arlt, R., Bonanno, A., & Licciardello, G. 2025, A&A, 702, A44
[14] Barrault, L., Mathis, S., & Bugnet, L. 2025b, A&A, 694, A225
[15] Ihallaine, S., Ballot, J., Lignières, F., et al. 2026, arXiv, 2605.22533